Polym. Bull. (2011) 66:541–549
DOI 10.1007/s00289-010-0334-6

ORIGINAL PAPER

Polymethacrylic acid/Na-montmorillonite/SiO_2 nanoparticle composites structures and thermal properties

Yan Bao · Jian-zhong Ma

Received: 18 May 2010 / Revised: 15 June 2010 / Accepted: 28 June 2010 /
Published online: 4 July 2010

Abstract In this article, polymethacrylic acid/Na-montmorillonite/SiO_2 nanoparticle (PMAA/Na-MMT/SiO_2) composites were prepared via in situ polymerization. Fourier transform infrared spectroscopy (FTIR) indicated that the polymerization of SiO_2 nanoparticle and MAA have been taken place. X-ray diffraction (XRD) results suggest that Na-MMT layers are exfoliated during the polymerization process. As evidenced by the transmission electron microscopy (TEM), the Na-MMT layers and SiO_2 nanoparticles exhibit good dispersion in the polymer matrix. It was found that the PMAA/Na-MMT/SiO_2 composite exhibit considerably enhanced thermal properties compared with the PMAA/Na-MMT.

Keywords Nanocomposite · Inorganic nanomaterial · Polymethacrylic acid

Introduction

Nanocomposites are a promising new class of technologically advanced materials, consisting of two or more phases in which at least one of its phases has one or more dimensions (length, width or thickness) in the nanometer size range, usually defined as 1–100 nm [1]. Nanocomposites show conspicuously enhanced mechanical,

Y. Bao (✉) · J. Ma
College of Resource and Environment, Shaanxi University of Science and Technology,
710021 Xi'an, China
e-mail: baoyan0611@126.com

Y. Bao · J. Ma
Key Laboratory of Chemistry and Technology for Light Chemical Industry, Ministry of Education,
710021 Xi'an, China

thermal, optical, and electro chemical properties compared to their neat or conventional composites [2–5].

Among various nanocomposites, much attention has been paid to polymer/Na-montmorillonite (Na-MMT) nanocomposites, in which nanometer-thick layers of clay are dispersed in polymers [6]. Calcagno et al. [7] prepared PET nanocomposites using montmorillonite with different organic modifiers. Nanocomposites of intercalated and exfoliated morphologies were obtained, and an average maximum distance between the platelets was observed in the intercalated morphology.

Another importantly used nanomaterial for the enhancement is SiO_2 nanoparticle [8, 9]. For instance, dramatical improvement of the strength, stiffness and thermal properties are reported for PA66-based nanocomposites containing surface-modified SiO_2 nanoparticle prepared by melt compounding [10].

Whether the nanocomposites still have high thermal stability and enhanced mechanical property, when two kinds of nanomaterials with different forms, layered and particle are incorporated into the polymer matrix? Peeterbroeck et al. [11] prepared EVA-based nanocomposites filled with both organoclays and purified multi-walled carbon nanotubes via direct melt blending. This new family of composites exhibits enhanced properties even at very low filler level.

In this work, the acrylic polymer-based nanocomposites filled with both clay and SiO_2 nanoparticles were prepared via in situ polymerization. The polymer matrix used in the present studies is polymethacrylic acid (PMAA). The structures and thermal properties of the obtained nanocomposites were examined by FT-IR, XRD, TEM, DSC and TGA.

Experimental

Materials

Na^+-montmorillonite (Na-MMT) was provided by Qing-he Chemical Factory, Zhangjiakou. Methacrylic acid (MAA), isopropyl alcohol and ammonium persulfate (APS) were all purchased from Tian-jin Chemical Reagent Factory. SiO_2 nanoparticle (RNS-D) was made by He-nan nanomaterial engineering center. Hexadecyl trimethyl ammonium bromide (CTAB) was purchased from San-pu Chemical Factory, Shanghai.

Preparation of PMAA/Na-MMT/SiO_2 composite

Na-MMT and dionized water were charged into a 250-mL three-necked round bottom flask equipped with a reflux condenser, a thermometer, and a magnetic stirring bar and stirred vigorously for 30 min. After MAA, 1631 and RNS-D fed into the flask for 30 min, the mixture was treated with ultrasound for 20 min and stirred for 5 h at 60 °C. Subsequently, the mixture was ultrasonically processed for 20 min. The aqueous solution of APS and isopropyl alcohol were fed into the flask at 70 °C. The reaction was kept at 80 °C for 2.5 h.

Characterization

The X-ray diffraction (XRD) patterns were obtained from a Japan Science 2200PC X-ray Diffractometer. The diffractograms were measured at 2θ, in the range 2°–10°, using a Cu-Kα incident beam ($\lambda = 0.1543$ nm), monochromated by a nickel filter. The scanning speed was 1°/min, and the voltage and current of the X-ray tubes were 40 kV and 20 mA, respectively. The morphology of the nanocomposite was observed by H-600 transmission electron microscopy (TEM). The Fourier transform infrared spectroscopy (FTIR) spectra were recorded on a 5DX FTIR using KBr pellets. The thermogravimetric analysis (TGA) was performed on a thermogravimetry differential thermal analysis 6300 apparatus. The differential scanning calorimetry (DSC) analysis was performed on an Exstar 6000 apparatus. The temperature program started in the range from 100 °C up to 150 °C at a heating rate of 10 °C/min under nitrogen atmosphere.

Results and discussions

FT-IR analysis

Figure 1 displays the differences among the structures of Na-MMT, SiO_2 nanoparticle and PMAA/Na-MMT/SiO_2 composite.

In the FT-IR spectrum (see Fig. 1A) of pristine MMT the broad band centered near 3400 cm^{-1} is due to the –OH stretching mode of the interlayer water. The overlaid absorption peak in the region of 1640 cm^{-1} is assigned to the –OH bending mode of adsorbed water. The characteristic peak at 1115 cm^{-1} is due to the Si–O–Si stretching and out of plane Si–O–Si stretching mode for montmorillonite. The band at 1035 cm^{-1} is assigned to the Si–O–Si stretching (inplane) vibration for layered

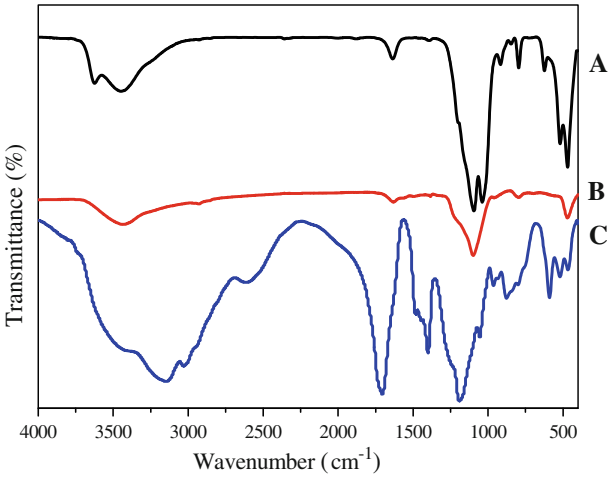

Fig. 1 FT-IR spectra (*A* Na-MMT, *B* SiO_2 nanoparticle, *C* PMAA/Na-MMT/SiO_2 composite)

silicates. The band in the region of 796 cm^{-1} is due to the Si–O–Al stretching mode for montmorillonite. The FTIR peaks at 522 cm^{-1} and 468 cm^{-1} are assigned to the Si–O–Al and Si–O–Si bending vibration, respectively [12, 13].

In FTIR spectrum of SiO_2 nanoparticle, the absorption peak 3442 cm^{-1} is affected by stretching vibration of Si–OH. The absorption peak 1638 cm^{-1} is stretching vibration of C=C. This is because the SiO_2 nanoparticle used in our research was modified by r-methacryloxy propyltrimethoxysilane as coupling agent. The vinyl groups were introduced onto surfaces of SiO_2. The weak absorption peak 1100 cm^{-1} belongs to stretching vibration of Si–O–Si.

The FTIR spectrum of PMAA/Na-MMT/SiO_2 composite shows that the intensity of the 3500–3200 cm^{-1} band is increased, along with a reduction of intensities due to Si–O and Al–O. The increase in intensity of the 3500–3200 cm^{-1} band reflects the increased hydrogen bonding between the lattice hydroxyls and polymer [14]. When the protons in the polymer were hydrogen bonded to the oxygen species of the Si–O and Al–O segments, Si–O and Al–O bonds were weakened and the tetrahedral symmetry of these moieties became distorted. At the same time, the –OH stretching frequencies were broadened and displaced to lower frequencies. These shifts also were attributed to the formation of hydrogen bonds. On the other hand, the peaks at 2940 and 2850 cm^{-1} were ascribed to the asymmetric and symmetric vibration of methylene groups [12]. The peaks at 1490–1410 cm^{-1} were bending vibration of methylene groups. The peaks at 1700 cm^{-1} were due to the C=O stretching mode of carboxyl. These results show that methacrylic acid was polymerized in the MMT inter-lamellar. The absorption peak 1638 cm^{-1} of C=C stretching vibration disappears, which explains that the polymerization of SiO_2 nanoparticle proceed expectedly.

XRD analysis

Shown in Fig. 2 are XRD diffraction patterns of Na-MMT, PMAA nanocomposites containing Na-MMT and Na-MMT/SiO_2 nanoparticle. A strong 001 characteristic diffraction peak of pristine MMT appeared at the 2θ value 7.02°, which corresponded to an interlayer d-spacing of 1.258 nm based on Bragg's equation (curve A).

Curve B is the result obtained for PMAA/Na-MMT. A diffraction peak at $2\theta = 2.61°$ is visible in this nanocomposite, corresponding to a d-spacing of 3.388 nm. This is because adequate amount of CTAB that enough to exchange all the Na^+ ions from the MMT interlammellar was introduced into the system before polymerization. Quaternary ammonium cations were intercalated into montmorillonite by ion exchange reaction under shearing. The interlayer d-spacing of MMT was enlarged. Then, the initiator was added into the solution. Methacrylic acids took place in situ polymerization in the interlayers of montmorillonite. Polymer chains were growing longer along with the proceeding of polymerization. Hence, the interlayer d-spacing of MMT was further enlarged.

Curve C gives typical XRD pattern of PMAA/Na-MMT/SiO_2 nanocomposite. The XRD results suggest that the Na-MMT layers are exfoliated as indicated by the disappearance of the Na-MMT diffraction peak in curve C [15–17]. Comparison of the XRD patterns of PMAA/Na-MMT/SiO_2 and PMAA/Na-MMT shows that the

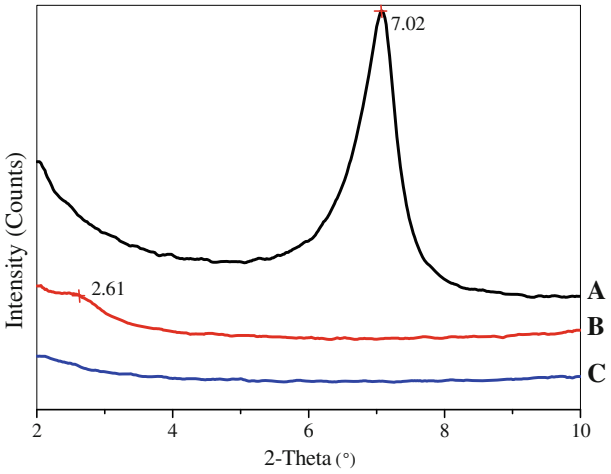

Fig. 2 XRD patterns (*A* Na-MMT, *B* PMAA/Na-MMT, *C* PMAA/Na-MMT/SiO_2)

introduction of SiO_2 nanoparticle has considerable influence on the interlayer d-spacing of montmorillonite. This is because SiO_2 nanoparticle used in this study is a kind of SiO_2 nanoparticle dealt by the silane coupling agent with vinyl groups. Radical copolymerization can be taken place between double bonds on the surface of SiO_2 nanoparticle and methacrylic acid. Therefore, the network crosslinked structure was formed between SiO_2 nanoparticle and polymethacrylic acid. The interlayer d-spacing of montmorillonite became larger until exfoliated as the molecular was bigger.

TEM analysis

In order to confirm the morphology of PMAA/Na-MMT/SiO_2 nanocomposite, TEM measurements were carried out (see Fig. 3). The dark slices stand for Na-MMT layers while the spherical dark particles are SiO_2 nanoparticle. The PMAA matrix appears as light region. The Na-MMT layers together with the SiO_2 nanoparticles show a good dispersion in the PMAA matrix.

Thermal properties

Figure 4 displays the DSC thermographs obtained for PMAA/Na-MMT and PMAA/Na-MMT/SiO_2 composites. The glass transition temperature (T_g) of the PMAA/Na-MMT/SiO_2 composite (T_g = 194.4 °C) is higher than that of PMAA/Na-MMT composite (T_g = 176.2 °C). According to the literature [18], the T_g of PMAA is 130 °C. The T_g relates to molecular mass of the polymer. The T_g is raised with the molecular mass of polymer increasing [19]. The molecular mass can be affected by the presence of filler in the in situ polymerization process. The lower molecular mass of polymer is obtained in the presence of filler [20, 21]. So the T_g should be decreased. But our experimental results contradict with it. Therefore, the increased

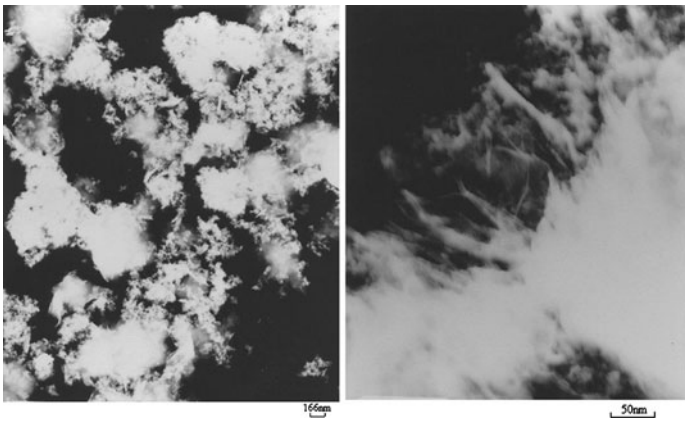

Fig. 3 TEM pictures of PMAA/Na-MMT/SiO_2 composite

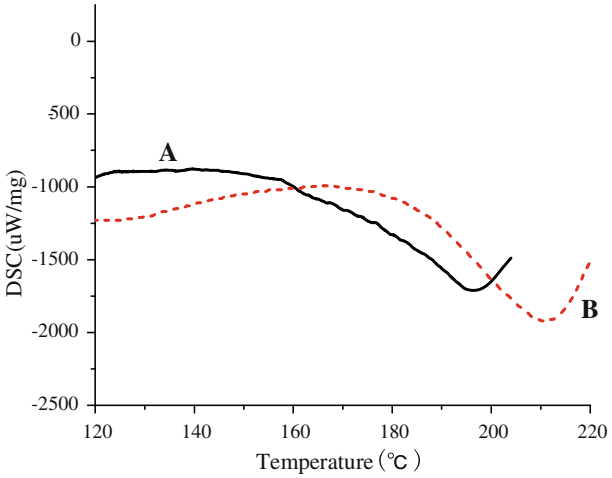

Fig. 4 DSC thermograms (*A* PMAA/Na-MMT, *B* PMAA/Na-MMT/SiO_2)

T_g resulted from the restricted segmental motions of the polymer chains at the organic–inorganic interface, due to the confinement of the polymer chains between the silicate layers, as well as the silicate surface–polymer interaction in the nanostructured hybrids [22–24]. On the other hand, the incorporation of SiO_2 nanoparticle interacts with polymer molecules to restrain the vertical molecule movement of PMAA.

Thermal stability of PMAA/Na-MMT/SiO_2 composite was evaluated using TGA in nitrogen atmosphere. For comparison, PMAA and PMAA/Na-MMT were also tested by TGA under the same conditions. The TGA data of weight change are shown in Fig. 5. Thermal degradation of pure acrylic polymers proceeds in three steps. The first step is initiated by scissions of head-to-head linkages (H–H),

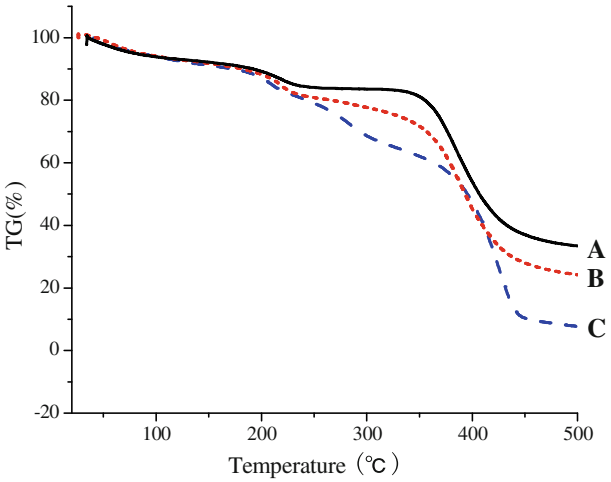

Fig. 5 TG curves (*A* PMAA, *B* PMAA/Na-MMT, *C* PMAA/Na-MMT/SiO_2)

the range between 160 and 240 °C. The second step (200–300) is initiated by scission at the vinylidene chain end units and the third step (above 300) by random scission within the polymer chain [25, 26]. This is because the first step and the second step are very close in temperature and are linked together in our research. Therefore, two steps of degradation process are observed.

The degradation curves for PMAA/Na-MMT/SiO_2 and PMAA/Na-MMT show a similar two-step degradation process as seen for PMAA, except that the first step exhibits poor thermal stability indicated by larger extent of weight loss associated with the first-step degradation in the temperature range of 160–300 °C. This difference may be due to the incorporation of SiO_2 nanoparticle and MMT. The free radical polymerization is hindered in the presence of filler. The number of vinylidene chain end units in the material is increased.

In the second step, PMAA/Na-MMT/SiO_2 composite exhibits an onset of thermal degradation of polymer main chains almost 30 °C higher than that of PMAA/Na-MMT and about 40 °C higher than PMAA. The noticeable increase in the decomposition temperature mainly results from the dispersed nanoscale silicate layers in matrix, which lead to the difficulty in heat conduction and acts as a mass transport barrier to the volatile products that generate during decomposition out of the material [27, 28]. Moreover, the clay has good thermal insulation effect and the incorporation of SiO_2 nanoparticle interacts with polymer molecules to restrain the vertical molecule movement of PMAA.

Conclusions

PMAA/Na-MMT/SiO_2 composites were prepared via in situ polymerization. FTIR indicated that the polymerization of SiO_2 nanoparticle and MAA has been taken place. X-ray diffraction (XRD) results suggest that Na-MMT layers are exfoliated

during the polymerization process. As evidenced by the transmission electron microscopy (TEM), the Na-MMT layers and SiO_2 nanoparticles exhibit good dispersion in the polymer matrix. It was found that the PMAA/Na-MMT/SiO_2 composite exhibit considerably enhanced thermal properties compared with the PMAA/Na-MMT.

Acknowledgements This research was supported by National 863 Foundation (No: 2008AA03Z311), scientific research plan of education department of Shaanxi province (No: 09JK344), scientific research group of Shaanxi University of Science and Technology (No: TD09-03) and the scientific research launching projects for doctor of Shaanxi University of Science and Technology (No: BJ09-01).

References

1. Soundararajah QY, Karunaratne BSB, Rajapakse RMG (2009) Montmorillonite polyaniline nanocomposites: preparation, characterization and investigation of mechanical properties. Mater Chem Phys 113:850–855
2. Salem N, Shipp DA (2005) Polymer-layered silicate nanocomposites prepared through in situ reversible addition–fragmentation chain transfer (RAFT) polymerization. Polymer 46:8573–8581
3. Usuki A, Hasegawa N, Kato M (2005) Polymer-clay nanocomposites. Adv Polym Sci 179:135–195
4. Zhou L, Yuan W, Yuan J et al (2008) Preparation of double-responsive SiO_2-g-PDMAEMA nanoparticles via ATRP. Mater Lett 62:1372–1375
5. Litina K, Miriouni A, Gournis D et al (2006) Nanocomposites of polystyrene-b-polyisoprene copolymer with layered silicates and carbon nanotubes. Eur Polym J 42:2098–2107
6. Meneghetti P, Qutubuddin S (2006) Synthesis, thermal properties and applications of polymer-clay nanocomposites. Thermochim Acta 442:74–77
7. Calcagno CIW, Mariani CM, Teixeira SR et al (2007) The effect of organic modifier of the clay on morphology and crystallization properties of PET nanocomposites. Polymer 48:966–974
8. Wang Y-P, Pei X-W, He X-Y et al (2005) Synthesis of well-defined, polymer-grafted silica nanoparticles via reverse ATRP. Eur Polym J 41:1326–1332
9. Hu J, Ma J, Deng W (2008) Properties of acrylic resin/nano-SiO_2 leather finishing agent prepared via emulsifier-free emulsion polymerization. Mater Lett 62:2931–2934
10. Xu X, Li B, Lu H et al (2007) The interface structure of nano-SiO_2/PA66 composites and its influence on material's mechanical and thermal properties. Appl Surf Sci 254:1456–1462
11. Peeterbroeck S, Alexandre M, Nagy JB et al (2004) Polymer-layered silicate–carbon nanotube nanocomposites: unique nanofiller synergistic effect. Compos Sci Technol 64:2317–2323
12. Patel HA, Somani RS, Bajaj HC et al (2007) Preparation and characterization of phosphonium montmorillonite with enhanced thermal stability. Appl Clay Sci 35:194–200
13. Uthirakumar P, Kim C, Nahm KS et al (2004) Preparation and characterization of new difunctional cationic radical initiator-montmorillonite hybrids. Colloid Surf A 247:69–75
14. Gunister E, Pestreli D, Unlu CH et al (2007) Synthesis and characterization of chitosan-MMT biocomposite systems. Carbohydr Polym 67:358–365
15. Urbanczyk L, Ngoundjo F, Alexandre M et al (2009) Synthesis of polylactide/clay nanocomposites by in situ intercalative polymerization in supercritical carbon dioxide. Eur Polym J 45:643–648
16. Suguna Lakshmi M, Narmadha B, Reddy BSR (2008) Enhanced thermal stability and structural characteristics of different MMT-Clay/epoxy-nanocomposite materials. Polym Degrad Stabil 93:201–213
17. Rao Y (2007) Gelatine/clay nanocomposites of improved properties. Polymer 48:5369–5375
18. Cao T, Liu Q, Hu J (2007) Synthesis, properties and applications of polymer emulsion. Chemical Industry Press, Beijing, p 257
19. Zaragoza-Contreras EA, Lozano-Rodrıguez ED et al (2009) Evidence of multi-walled carbon nanotube fragmentation induced by sonication during nanotube encapsulation via bulk-suspension polymerization. Micron 40:621–627
20. Uthirakumar P, Nahm KS, Hahn YB et al (2004) Preparation of polystyrene/montmorillonite nanocomposites using a new radical initiator-montmorillonite hybrid via in situ intercalative polymerization. Eur Polym J 40:2437

21. Yu YH, Lin CY, Yeh JM et al (2003) Preparation and properties of poly(vinyl alcohol)-clay nanocomposite materials. Polymer 44:3553
22. Shi X, Gan Z (2007) Preparation and characterization of poly(propylene carbonate)/montmorillonite nanocomposites by solution intercalation. Eur Polym J 43:4852–4858
23. Doh JG, Cho I (1998) Synthesis and properties of polystyrene organoammonium montmorillonite hybrid. Polym Bull 41(5):511–518
24. Fu XA, Qutubiddin S (2001) Polymer-clay nanocomposites: exfoliation of organophilic montmorillonite nanolayers in polystyrene. Polymer 42(2):807–813
25. Huskic M, Igon MZ (2007) PMMA/MMT nanocomposites prepared by one-step in situ intercalative solution polymerization. Eur Polym J 43:4891–4897
26. Hirata T, Kashiwagi T, Brown JE (1985) Thermal and oxidative degradation of polymethyl methacrylate: weight loss. Macromolecules 18:1410–1418
27. Shi X, Gan Z (2007) Preparation and characterization of poly(propylene carbonate)/montmorillonite nanocomposites by solution intercalation. Eur Polym J 43:4852–4858
28. Li S, Yang J-T, Lin G-Y et al (2007) Crystallization and thermal properties of polyamide 6 composites filled with different nanofillers. Mater Lett 61:3963–3966